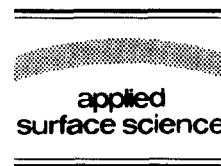




ELSEVIER

Applied Surface Science 96–98 (1996) 149–153



Monitoring stress power during high-power pulsed laser–material interactions

Mark A. Shannon ^{a,*}, Richard E. Russo ^b

^a *Department of Mechanical Engineering, University of Illinois at Urbana-Champaign, Urbana, IL, USA*

^b *Lawrence Berkeley Laboratory, Berkeley, CA, USA*

Received 22 May 1995

Abstract

High-power pulsed laser–material interactions are monitored with acoustic measurements of mechanical stress power. At laser intensities above 10^8 W/cm², an explosive, plasma forming interaction occurs between the laser beam and the solid target, ablating material away. Stresses in the target caused by the laser ablation can be very large, which for short pulsed laser ablation can make mechanical transport of energy significant. Experimental work is conducted to study the affect of laser intensity on stress power in the target and that carried by pressure waves in the surrounding gas medium. 30 ns excimer and 35 ps Nd:YAG lasers are used to ablate Al and Cu targets, and the resulting stresses are recorded by different types of transducers. The nanosecond results show that gas ionization breakdown can be detected through the stress power, and that the power measured follows a near quadratic dependence on the incident energy. Variations in the ratio of the shock power in air to the stress power in the target shows that plasma shielding of the laser beam can be monitored using the mechanical stress power. Differences in plasma shielding during pico-second ablation of copper in Ar versus He are shown using stress power monitoring.

1. Introduction

With the advent of processes such as laser-sampling for chemical analysis, pulsed-laser annealing, microfabrication, and pulsed-laser deposition of thin films, there has been a growing need to monitor laser-energy coupling to a solid. The coupling of laser energy to solids can occur via different transport phenomenon: thermal, chemical, mechanical, and electromagnetic. At power densities above about 10^8 W/cm² significant dissociation and ionization of the molecules and atoms in the medium and target

material may occur, further complicating the laser energy coupling. With high-power laser ablation of a solid, plasma generation may shield the direct laser intensity from the reaching the target [1]. The subsequent radiation by the plasma heats the material over a much longer period, perhaps increasing undesirable thermal processes. Yet other applications may show improved results if a plasma is generated and fully ionized. In all cases, the amount of laser energy that is coupled to the target is highly variable depending on laser's power, wavelength, pulse duration, and the target's material and optical properties, as well as the surrounding medium. Moreover, the energy coupling can be very sensitive to small changes in surface properties and morphology, making prediction very

* Corresponding author.

difficult. Due to the complicated partitioning of energy during high-power laser–material interactions, a method is desired to monitor laser energy coupling that implicitly includes different mechanisms.

During high-power, short-pulsed laser–material interactions very high stresses result from thermal expansion and phase-change, as well as recoil momentum and shock waves induced by the dynamics of the ablation products leaving the target at high velocities [2]. Brittle fracture, plastic deformation, and spallation of normally ductile materials have all been observed to occur during high-power laser–material interactions. Also, pressures greater than 10,000 atm have been measured above the target. However, high stresses per se do not reveal how much laser energy is coupled mechanically to the target.

Laser-induced stresses have been used extensively to probe laser–material interactions: researchers have used shock wave detection [3], and stress wave response in the target [4] to detect the onset of ablation. There is also a large amount of literature dating back to the 1960's on the momentum recoil [5], shock pressures [6], mechanical response to shock [7], and stress waves generated by lasers [8]. But to date, the rate at which energy carried by the mechanical stress propagating through a target has not been addressed to monitor laser energy coupling with materials. Moreover, the extent to which energy is carried mechanically and its effect in high-power laser–material interactions is unknown at this point.

Investigating stress power in laser–material interactions is interesting in itself, but stress power in the far field can be used to monitor complicated laser energy coupling to a solid target [9]. Specifically, this paper will present the underlying theory and method of measuring stress power, the initial results of stress power measured in and above the target, and discuss the effects of gas ionization breakdown and plasma shielding on the stress power measurements.

2. Theory

In thermomechanics, a general equation that balances energy includes volumetric and surface heat transfer, potential and internal energies, and internal

heat generation. Combining the rate of mechanical work with the rate of heat that is supplied to the body, the sum must equal the rate of change of kinetic energy plus heat density plus the potential energy. Expressing the energy balance in terms of the contact \mathbf{t} and body \mathbf{b} forces, Helmholtz free energy potential ψ , entropy density per unit mass η , absolute temperature θ , external supply of heat r , and the normal heat flux $\mathbf{h} = \mathbf{q} \cdot \hat{\mathbf{n}}$ gives [10]

$$\int_{\Omega_B} (\mathbf{t} \cdot \mathbf{v} - h) da + \int_B \rho(r + \mathbf{b} \cdot \mathbf{v}) dV \\ = \frac{d}{dt} \int_B \rho \left(\frac{1}{2} \mathbf{v} \cdot \mathbf{v} + \psi + \eta \theta \right) dV, \quad (1)$$

where \mathbf{v} is the velocity of a material point, and V is volume. The internal energy density e is $e = \psi + \eta \theta$. Locally, the power carried mechanically in (1) has an explicit dependence on heat transfer and the rate of change of internal energy \dot{e} , such that

$$P = \rho r - \text{div } \mathbf{q} - \rho \dot{e} \quad (2)$$

where ρ is the density, r is all heat sources, and $\text{div } \mathbf{q}$ is the divergence of the heat flux [10]. Note that e includes all the factors that affect the internal energy, such as chemical reactions, vibrational and electronic excitations, as well as kinetic and electromagnetic energies that can arise during laser ablation. Of note is that (2) gives a direct measure of when stress power becomes significant in short pulsed laser–material interactions. The stress power, P , is defined as

$$P = \mathbf{T} \cdot \mathbf{L} \quad (3)$$

where \mathbf{T} is the Cauchy stress tensor $\tau_{ij} \mathbf{e}_i \otimes \mathbf{e}_j$, and \mathbf{L} is the velocity gradient tensor $\partial \mathbf{v} / \partial \mathbf{x} = v_{i,j} = \partial v_i / \partial x_j$ ($i, j = 1, 2, 3$). For a body, the summation $\tau_{ij} v_{i,j}$ describes the mechanical power instantaneously in each elemental volume. Note that P can be dissipative. Depending on the material and the dissipative mechanisms, the stress power can be thermalized, further heating the body, or could lead to raising the kinetic energy of fracture and/or particles. For most interactions, P/ρ is very small with respect to the incident laser power, given by r . However, if P is of the order of ρr , then the stress power is a significant mode of energy transport in the target.

The stress power in (3) can be large if the stress

amplitudes times the velocity gradients are large. High stresses applied over a long time do not give rise to high stress power. However, if the target is stressed over a very short time period such that the change in velocity over a short distance is large, then high stress power can result. *High-power, short-pulse laser–material interactions give rise to precisely the type of loading which creates high stress power.* To illustrate, consider a loading σ of 10^{10} Pa caused by a 30 ns 0.5 J laser pulse with a 50 μm laser spot size and an average power of 17 MW. The energy travels at a speed c , which is at least the elastic wave speed c_0 of the material. Assuming a one-dimensional elastic wave propagation, the laser spot area times the maximum distance, $x_1(\text{max}) = ct$, gives an average value for L as

$$L \approx \frac{\Delta v_1}{\Delta x_1} \approx \frac{c}{ct} = \frac{1}{t} = \frac{1}{30 \cdot 10^{-9} \text{ s}} = O(10^7) \text{ s}^{-1}. \quad (4)$$

Here, $P \approx \sigma$, $\Delta v_1/\Delta x_1$ is on the order of 10^{17} W/m^3 , and the effected volume \mathcal{V} is about 10^{-13} m^3 for a wave speed $c_0 \approx 5000$ m/s . $P\mathcal{V}$ for this case is roughly 1 MW, which is a small but appreciable fraction of the laser power. If the material in the near field of the ablation becomes fully compressed so c greatly exceeds c_0 , $P\mathcal{V}$ would be limited by the partition of the laser energy between plasma heating, thermal heat transfer, and the dissipative deformation processes.

3. Experimental

A series of experiments were carried out to consider separately the effect of energy, intensity, spot size, and gas atmosphere during laser ablation of aluminum and copper targets. The mechanical response of the ablation was detected with three different types of transducers to identify the density wave in the ambient medium, and the longitudinal, shear, and surface waves in the target. As shown in Fig. 1, a pulsed-laser strikes a solid target mounted on an acoustic emission transducer with a -3 dB frequency response from 10 kHz to 18 MHz which transmits the resulting stress wave to a Tek602a 2 Gsample/s oscilloscope. A 1 MHz surface-wave

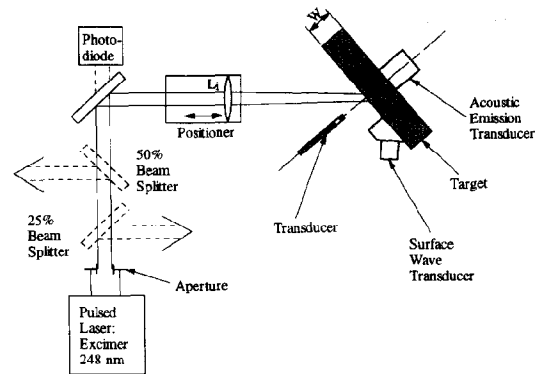


Fig. 1. Schematic of the stress power experimental system. Three different transducers record the stress waves emanating from the laser–material interaction.

transducer records the Rayleigh wave, and above the target is a Valpey–Fisher model VP-1093 0 to 1.2 MHz transducer linear up to approximately 2000 atm that records the pressure wave emanating from the pulsed-laser interaction. The peak frequencies and pressures recorded in the far field were all well within the limits of the transducers.

Note that acoustic emission monitoring of stress power provides a measure in the far field of changes in stress power near the laser–material interaction site. The transducers employed in the measurements produce a voltage that is a scalar quantity proportional to the average stress in the element volume. Dividing this average stress by the volume gives a stress per unit volume that is changing in time. For an averaged scalar stress, the stress power in (3) is $2C\sigma\dot{\sigma}$ where C is a proportionality constant, and σ is the average stress in the transducer. Therefore, the average stress power at any time in the transducer is a function of the stress and the rate of change in the stress. The average power contained in the acoustic emission signal, $s(t)$, is calculated by integrating in the frequency, f , domain, such that

$$\begin{aligned} \int |S(f)|^2 df &= 2C \int f \Sigma(f) \Sigma^*(f) df \\ &= 2C \int f \Sigma^2(f) df \end{aligned} \quad (5)$$

where $s = \sqrt{C} \sigma$, $\Sigma(f)$ is the Fourier transform of $\sigma(t)$, and Σ^* is the complex conjugate [11].

4. Results and discussion

The log of the calculated signal powers for 30 ns, 248 nm excimer laser ablation of a 2 mm Al target over 8 different spot sizes are shown in Fig. 2(a) versus the log of the intensity. The signal power, and thus P , grows according to the power law, $P = cI^m$, where the values for c and m are shown. For the first five runs, the exponent m averages 2.46, and for the final 3 runs m average 1.76. Therefore, the stress power has a near quadratic dependence on intensity for a given spot size. A quadratic dependence is

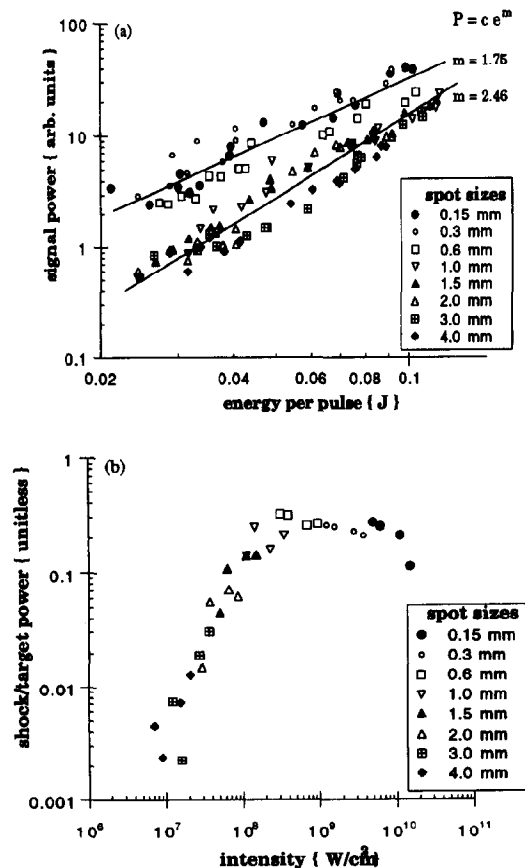


Fig. 2. In (a) the stress power is plotted as a function of energy per pulse by varying laser spot sizes at four different laser powers for each size beam for an Al target being ablated by a 30 ns excimer laser at 248 nm. Different slopes are due to gas ionization breakdown. In (b), the ratio of the stress power in air over the target power is plotted versus the incident intensity at the surface of an Al target.

expected if the thermal expansion behaves linearly elastic *and* the pressure increases linearly with laser energy. Thus, the stress power combined with measurements of pressure and temperature can probe the nature of a high-power laser-material interaction.

The other point of interest in Fig. 2(a) is that for spot sizes less than 1 mm, P starts at a baseline an order of magnitude higher than for those ≥ 1 mm, and then approaches the values reached by the larger spot sizes. The baseline shift is due to the creation of a shock wave caused by ionization breakdown. The lower rate of increase (1.7 versus 2.4) with laser energy for intensities which cause initial breakdown is likely due to plasma shielding of the laser beam.

The explicit affect of plasma shielding for excimer laser ablation can be seen in Fig. 2(b) in a plot of the ratio of the stress power in the shock wave of the expanding plume to the stress power in an Al target. At about $3 \times 10^8 W/cm^2$ incident intensity, the ratio of shock to target stress power rolls off and it declines above $10^{10} W/cm^2$. Laser-induced breakdown of gases can occur at about $10^8 W/cm^2$ above a metallic target [12,13]. Above $10^{10} W/cm^2$, the plume above the Al surface is observed to be a highly-ionized plasma. The stress power ratio shows the same behavior since the onset of plasma shielding reduces the ablated mass driving the shock front, yet increases the temperature and recoil of the ejected particles. The result of plasma shielding is that more power is coupled mechanically to the target, with respect to that carried by the ablation products.

The effect of gas composition and pressure on laser energy coupling for single nano- and pico-second UV laser pulses can be seen in Fig. 3. For 30 ns excimer laser ablation of copper targets at 248 nm at 9 mJ and 1 mm diameter spot size ($4 \times 10^7 W/cm^2$), the effect of varying pressure from high-vacuum to one atmosphere has little effect on the stress power, as seen in Fig. 3 for Ar (a) and He (b). For 35 ps Nd:YAG ablation at 266 nm at 9 mJ and $3 \times 10^{10} W/cm^2$, however, a difference of up to 5 times is observed between Ar and He atmospheres as the pressure increases to 1 atm. The strong scattering in the single shot ps Ar data is likely due to the highly non-linear dependence on fluctuations laser power near the plasma shielding threshold. It has previously been observed [14] that large differences in laser sampling for chemical analysis occurs in Ar versus

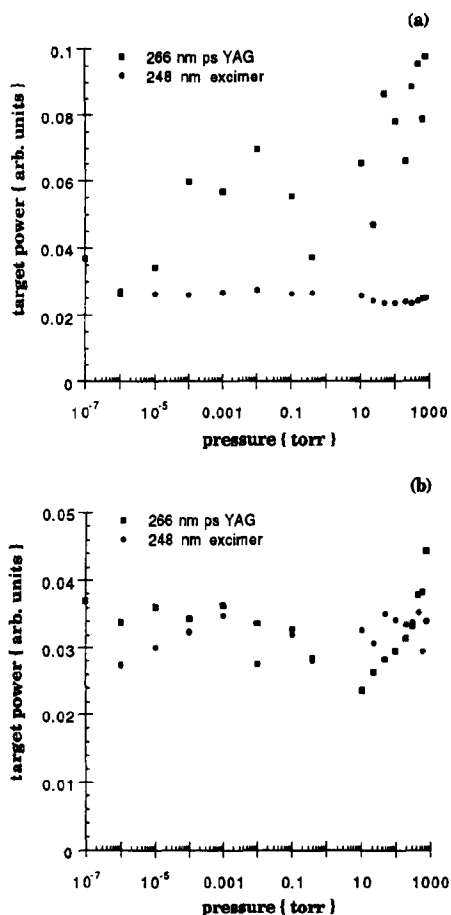


Fig. 3. Effect of gas composition and pressure on stress power in a 1 mm thick copper target for nano- and pico-second UV laser pulses at 9 mJ/pulse for a 1 mm dia. laser spot size in an Ar (a) and He (b) atmosphere.

He atmospheres for ps ablation, but relatively small differences occurred for ns ablation, presumably due to differences in plasma shielding between the gases. These stress power results show that more laser

energy is coupled mechanically to the target in Ar versus He due to an increase in energy absorbed by the Ar medium versus He as pressure increases, which is consistent with plasma shielding.

These examples illustrate the value of monitoring the stress power generated during high-power laser–material interactions for probing laser energy coupling. Future efforts must be undertaken to better understand the partitioning of energy via mechanical stress power, particularly with respect to laser pulse width, wavelength and intensity, plasma formation, and the dynamics of the plume.

References

- [1] C.R. Phipps and R.W. Dreyfus, in: *Laser Ionization Mass Analysis*, Eds. A. Vertes, R. Gijbels and R. Adams (Wiley, New York, 1993).
- [2] D.B. Geohegan, *Thin Solid Films* 220 (1992) 138.
- [3] G. Koren, *Appl. Phys. Lett.* 51 (1987) 569.
- [4] P.E. Dyer and R. Srinivasan, *Appl. Phys. Lett.* 48 (1986) 445.
- [5] G.A. Askar'yan and E.M. Moroz, *Sov. Phys. JETP* 16 (1963) 1638.
- [6] R.E. Beverly III and C.T. Walters, *J. Appl. Phys.* 47 (1976) 3485.
- [7] J. Fournier, P. Ballard, P. Merrien, J. Barralis, L. Castex and R. Fabbro, *J. Phys. III France* 1 (1991) 1467.
- [8] A. Neubrand and P. Hess, *J. Appl. Phys.* 71 (1992) 227.
- [9] M.A. Shannon, PhD dissertation, University of California (Berkeley, CA, 1993).
- [10] A.C. Green and P.M. Naghdi, *Proc. R. Soc. London A* 432 (1991) 171.
- [11] H.J. Weaver, *Applications of Discrete and Continuous Fourier Analysis* (Wiley, New York, 1983).
- [12] V. Kumar and R.K. Thareja, *Laser and Particle Beams* 10 (1992) 109.
- [13] C. Boulmer-Leborgne, J. Hermann and B. Dubreuil, *Plasma Sources Sci. Technol.* 2 (1993) 219.
- [14] X.L. Mao, W.T. Chan, M.A. Shannon and R.E. Russo, *J. Appl. Phys.* 74 (1993) 4915.